SOLID-STATE ELECTRONICS

Experimental investigation of a resistive single-quantum logic structure

A. N. Vystavkin, V. K. Kaplunenko, V. P. Koshelets, K. K. Likharev, V. V. Migulin, O. A. Mukhanov, G. A. Ovsyannikov, V. K. Semenov, and I. L. Serpuchenko

Institute of Radio Engineering and Electronics, Academy of Sciences of the USSR, Moscow

(Submitted July 6, 1987)

Zh. Tekh. Fiz. 59, 26–34 (December 1989)

A test structure for the verification of the main components of a recently proposed resistive single-quantum logic has been developed and experimentally investigated. The structure includes a single-quantum pulse generator, a segment of neuristor line for their transmission, amplifiers for the multiplication and combining of these pulses, and also a universal NOR gate. The functional circuits were verified by measuring the constant voltages $\overline{V}$ on various elements of the structure, the magnitudes of which are connected with the frequencies of the information pulses passing through them by the Josephson relation $f=\overline{V}/\Phi_0$. The structure was assembled from niobium-film based superconducting junctions, with a minimal area of 10×10 μm^2 and critical current density $j_c = 2\text{–}5\times 10^2$ A/cm², shunted by external resistors with resistances of ~ 1 Ω, which ensured small values of the normalized capacitance of the junctions ($\beta_c \leq 1$) and relatively large values of the characteristic voltage $I_cR_N \simeq 200\text{–}500$ μV. Tests demonstrated the workability of the entire test circuit at clock frequencies up to 30 GHz, and the logic element itself at clock frequencies up to 48 GHz.

INTRODUCTION

Recently great interest has been shown in digital Josephson structures in which information is stored in the form of single quanta of the magnetic flux Φ_0, and is transmitted in the form of short voltage pulses with area

$$\int V(t)\,dt = \Phi_0. \qquad (1)$$

In contrast with other known logic circuits based on single quanta of the magnetic flux (using transmission lines based on distributed junctions,[1] shift registers of magnetic-shuttle type[2] or paramagnetic quantrons[3,4]), in the structure under consideration here the single-quantum pulses are transmitted over resistive (as opposed to purely inductive) lines, after which they are regenerated by the subsequent circuit elements to their nominal level (1). Such an operating principle presents the possibility of transmitting impulses over as long a distance as desired by regenerating them by means of special amplifiers. Single Josephson junctions with small capacitance ($\beta_C \lesssim 1$), biased by a constant current I_0 smaller than the critical current I_C, can play the role of such amplifiers (it is possible to use still more complicated structures with the same junctions[5–8]).

The first device to use this principle of information coding was a binary counter for a precision analog–digital converter. This specialized functional device was proposed by Silver and coworkers[9] and later realized by Silver et al.[5] and by Hamilton and Lloyd,[10] who demonstrated its ability to function at frequencies up to 100 GHz.

The success which has been achieved in the development of these very simple elements has transformed the problem of constructing more complicated logic devices into one of current interest. Silver et al.[5] noted that it is possible to build an AND gate by using a two-contact interferometer based on low-capacitance junctions. However, the proposed gate is unrealizable in practice since its operation is based on the temporal coincidence of ultrashort (picosecond) pulses. Moreover, even the realization of a reliable AND gate is not sufficient for the creation of a complete system of logical functions.

In Refs. 7, 8, and 11 it was shown that such a complete system can be realized if one uses a more suitable principle for the representation of digital information. In the elements of this system the single-quantum pulses are transmitted over two lines. The first of these transmits the information pulses and the second, the clock pulses, and the logical 1 is represented by the presence, and the logical 0, by the absence, of an information pulse between two successive clock pulses. Such a way of representing information makes it possible to create a complete system of logic structures, including the NOR gate, the most critical for the development of digital circuits based on Josephson junctions. Numerical modeling of such structures has shown[7,8,11] that even using Josephson junctions with characteristic voltage $V_C = I_CR_N \approx 500$ μV such resistive single-quantum circuits with constant current feed can have a clock frequency of up to 60 GHz, which is considerably higher than that of any previously known logic structure.

The aim of the present effort was to carry out experimental investigations of the basic components of a resistive single-quantum logic, including the NOT gate, which in this logic practically coincides with the NOR gate, which is sufficient for the realization of any logical operation.

1. THE IDEA OF THE EXPERIMENT

Figure 1 shows a block diagram of the experimental logic structure. Periodic single-quantum pulses from the generator G are regenerated and multiplied by a buffer cascade (amplifier–pulse

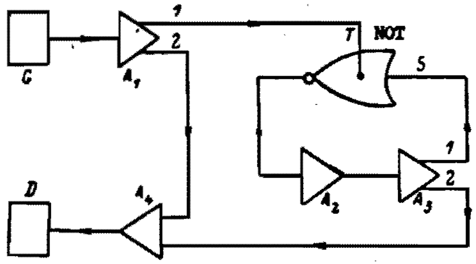

FIG. 1. Block diagram of the investigated resistive single-quantum test structure, which consists of a generator G, amplifier–pulse stretchers A_1 and A_2, amplifier A_3, amplifier–combiner A_4, detector D, and NOR gate.

stretcher) A_1, pulses from the output 1 of which arrive at the NOT gate as clock pulses. If in the interval between two of these clock pulses a similar pulse does not arrive at the information input S of the NOT gate, then the clock pulse passes through to the output of the gate. The output pulse is held back in the amlifier A_2, multiplied by the amplifier A_3, and proceeds from output 1 of amplifier A_3 to the information input S of the NOT gate. If the delay time of this circuit is less than the period of the clock pulses, the following clock pulse will not pass through to the output of the gate. Thus, when the entire circuit is functioning normally, the frequency of the pulses passing through the amplifier A_2 is half the initial frequency f_0 of the pulses passing through the amplifier A_1. These two series of pulses are combined by the amplifier A_4, and thus pulses arrive at the detector D with frequency $(3/2)f_0$.

2. BASIC CIRCUIT

Figure 2 shows the basic circuit of the investigated logic structure. Auxiliary circuit elements such as resistors, shunting Josephson tunneling junctions, inductances (which are essential to connect the elements), and large-area Josephson junctions (which provide superconducting contacts between the film layers of the circuit) are not shown. Also not shown is the resistive divider of the total feed current I_{feed}, which provides the bias currents, shown in Fig. 2 by arrows, in addition to the generator current I_{in}, which is extracted separately. In addition to this, there was the possibility of independently tuning each of the Josephson circuit elements.

For ease of visualization of the processes taking place in the operation of the circuit, Fig. 3 shows the basic voltage traces, which were obtained by numerical modeling with the help of the program KOMPASS.[12]

The generator G consists of a Josephson junction J_0 to which a constant voltage V_0 is applied with the help of the inductance L_0 and the resistance R_0. This voltage causes the junction J_0 to generate single-quantum pulses (1) with frequency $f_0 = V_0/\Phi_0$. These pulses arrive at the amplifier–pulse stretcher A_1 (Fig. 3a), which consists of Josephson junctions J_1 and J_{11}, the constant feed current of which is less than the critical value. The single-quantum pulse arriving at the junction J_1 increases the current through it to a value greater than critical, which causes a change of 2π in the Josephson phase difference at the junction J_1, i.e., pulse generation takes place. The constant bias current through the transition J_{11} is chosen in such a way that this junction provides unidirectional pulse propagation from J_1 to the amplifier–combiner A_4 (junction J_7). Similar pulses through the resistor R_{12} arrive at the clock input of the NOT gate.

The NOT gate consists of the two-contact interferometer (circuit elements J_2, J_3, L_2, L_3) of the junction J_4 and shunt G_1. For certain values of the bias currents I_3 and I_2 the interferometer possesses two stable states which differ in the direction of the current circulating in the ring of the interferometer. Depending on the state of the interferometer, the current in the junction J_3 is either close to or less than the critical value. Therefore, the clock pulse acting on the pair of successively connected junctions J_3 and J_4 will

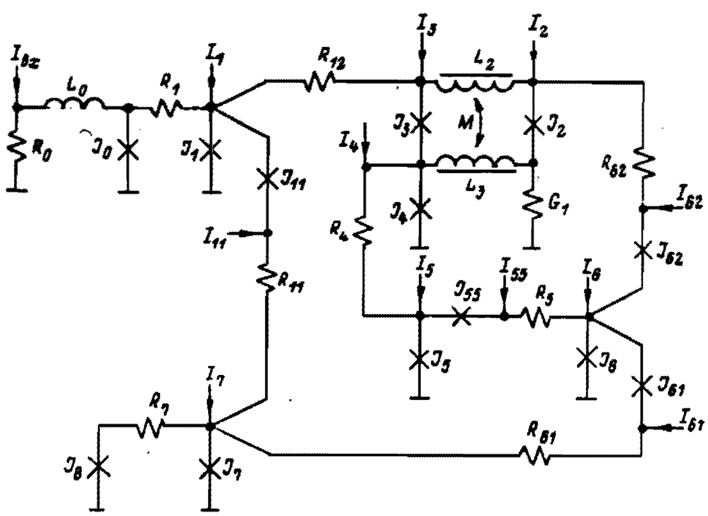

FIG. 2. Basic circuit of the test structure. The arrows indicate the points at which the feed currents were fed in, which were also the points at which the constant voltages $\bar{V}_i$ were measured.

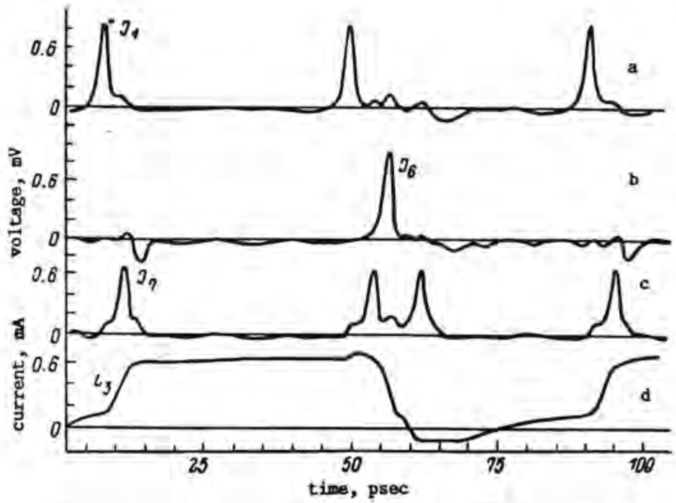

FIG. 3. Time courses of the voltages obtained by numerical modeling for the Josephson junctions J_1, J_6, and J_7, and of the current flowing through the inductance L_3. In the calculations the following parameter assignments were made: $I_{c0} = I_{c1} = I_{c6} = I_{c7} = 1$ mA, $I_{c4} = I_{c5} = 0.75$ mA, $I_{c11} = I_{c2} = I_{c3} = I_{c55} = I_{c61} = I_{c62} = 0.5$ mA, $I_1 = I_{11} = I_3 = I_{61} = I_{62} = I_5 = 0.4$ mA. $I_7 = 0.93$ mA, $I_{55} = I_4 = I_2 - I_4 = 0.2$ mA, $I_3 - I_2 = 0.28$ mA, $R_1 = R_{12} = R_{11} = R_5 = 0.2$ Ω, $R_0 = 0.3$ Ω, $R_7 = 0.5$ Ω, $R_{61} = 1/G_1 = R_4 = 0.25$ Ω, $R_{62} = 0.1$ Ω, $L_0 = 8$ nH, $L_2 = L_3 = 11$ pH, and $M = 0.6L_2$. The voltage on the generator $\bar{V}_0$ was 50 μV, corresponding to a Josephson generation frequency $f \simeq 25$ GHz.

cause a 2 π-jump in the phase difference of one of the junctions and will thereby either change the state of the interferometer or pass through to the output of the NOT circuit (Fig. 3d).

This output pulse arrives through the resistor R_4 at the amplifier A_2 formed by the junctions J_5 and J_{55}, is expanded by the amplifier–pulse stretcher A_3 (junctions J_6, J_{61}, and J_{62}) and is then passed through the resistor R_{62} to the information input of the inverter (Fig. 3b), and through R_{61} to the combining amplifier A_4. This amplifier consists of Josephson junction J_7, which is biased by the constant current $I_7 < I_c$ and loaded through the resistor R_L on the unbiased junction J_L. This node serves as a combiner of the pulses arriving through the resistors R_{11} and R_{61} (Fig. 3c), for their absorption in the circuit R_L, J_L, and also as the detector D.

The single-quantum pulses (1) have very short duration and very small amplitude (in our case respectively 3 psec and 0.8 mV), because of which quite complicated experimental instrumentation is required for their direct observation.[13] In the present paper we have used a technique commonly applied in the investigation of single-quantum Josephson structures:[5,10] to determine the pulse repetition frequency of the single-quantum pulses f_i through the given junction, a measurement is made of the constant voltage on it $\bar{V}_i = \Phi_0 f_i$. Thus, an indication of the correct functioning of the investigated structure is that in some voltage interval of the generator the following relations are fulfilled at the indicated points of the circuit:

$$\begin{aligned} &V_0 \text{ at } J_1,\ J_{61},\\ &{}^1/_2 V_0 \text{ at } J_2 - J_6,\ J_{11},\\ &{}^3/_2 V_0 \text{ at } J_7. \end{aligned} \qquad (2)$$

3. TECHNIQUE OF FABRICATION AND CONSTRUCTION OF THE TEST STRUCTURE

Figure 4 shows photographs of the investigated structure before and after formation of the upper electrode. The structure was assembled with a minimal line width of 10 μm and using only two superconducting layers. This dictated the necessity of the extensive use of auxiliary large-area Josephson junctions to carry the working currents from one layer to the other. The relatively large superconducting inductances L_2 and L_3 were fabricated in the form of narrow stripes on the upper and lower electrodes, respectively, and were located above the gaps in the opposing electrodes; here the mutual location of the stripes provided the required inductive coupling between the inductances ($M \approx 0.6L_2$). Nb–Al_2O_3–Nb structures were used as the Josephson junctions.[14,15]

A schematic section of a small segment of the investigated structure is shown in Fig. 5. The samples were prepared on a silicon substrate 1, covered by a protective layer 2 of Al_2O_3 of thickness ~200 nm. Molybdenum films of thickness ~100 nm with resistance per square $R_{\square}^{4.2} \approx 1$ Ω, obtained by rf cathode sputtering, were used as the shunts. The geometry of the shunts was formed with the help of chemical etching: for the subsequent layers the method of "explosive" photolithography was used. The lower 4 and upper 5 niobium electrodes, of thickness 200 and 400 nm, respectively, were deposited by magnetron sputtering. As the insulator 6 a double layer of silicon monooxide was used which had a total thickness of 300 nm, and in which windows were formed for the working tunneling Josephson junctions 7, whose cross-sectional areas were 100, 150, and 200 μm², respectively, and also for the auxiliary large-area junctions, which provided a connection from the one layer to the other. The tunneling barrier was formed by the method of thermal oxidation[15] of a thin film of Al sputtered onto the lower electrode after being clean in an rf discharge.

The junctions thus fabricated had a critical current density $j_c = 0.2$-0.5 kA/cm², small leakage currents ($V_m > 10$ mV), and did not change their characteristics during multiple thermocycling. The spread in the critical currents over the substrate did not exceed ±5%.

4. RESULTS OF EXPERIMENT

All of the experiments with the test circuit were carried out at the temperature T = 4.2 K. Before tuning the circuit as a whole, it was deemed necessary to check that the individual parts were working properly. First it was necessary to verify the very fact of transmission of single-quantum pulses from one junction to the other. An example of such a verification is shown in Fig. 6. Autonomous current–voltage characteristics of junctions a and b are shown in Fig. 6, curve 5. The remaining characteristics were obtained for fixed current I_b through junction b and temporal scanning of the current I_a through junction a. For the case in which the current I_b was above critical (Fig. 6, 1), a region of mutual synchronization of the jucntions is observed in the current–voltage characteristic (see the review Ref. 16). If I_b is less than the critical current (Fig. 6, curves 2-4), then the constant voltage on junction a appears simultaneously with the voltage on junction b as soon as the current

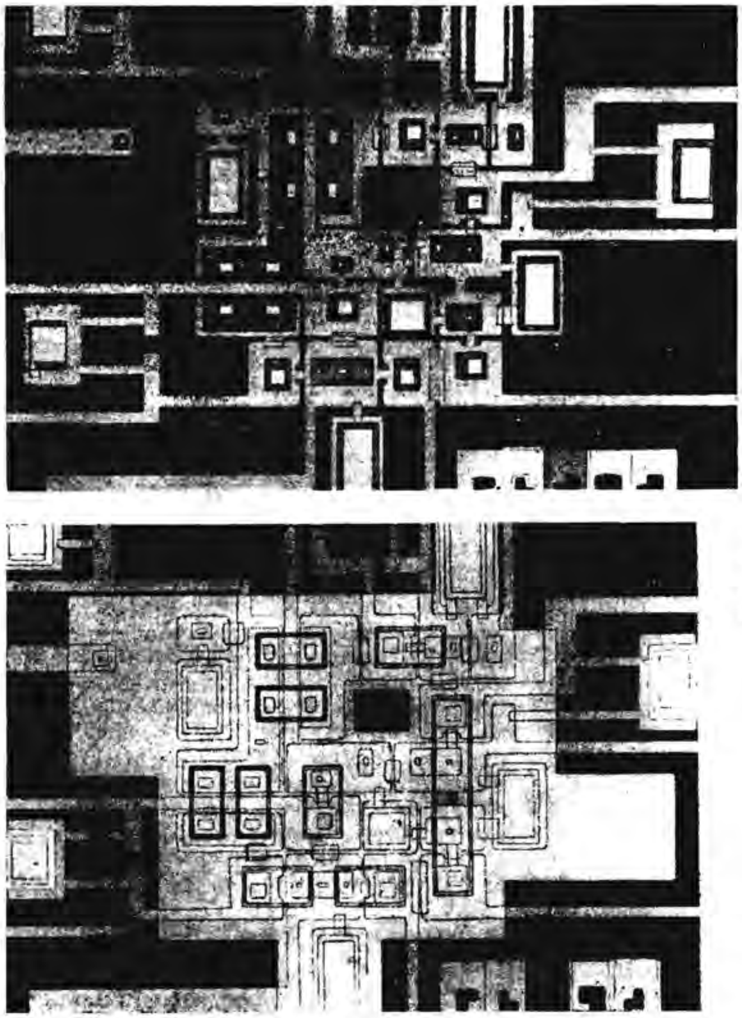

FIG. 4. Photographs of the investigated structure before the formation of the upper electrode (a) and after deposition of all the layers (b).

I_a exceeds the corresponding critical value. This phenomenon is naturally explained by the fact that the pulses being generated in junction a are transmitted to junction b and regenerated by the latter. It is clear from Fig. 6 that the range of such regeneration $\delta I_a/I_c \approx 50\%$ is observed at $I_b \approx 0.85$ mA, which is close to the calculated value $I_b \approx 0.8I_c$.

The tuning of the entire test structure was carried out in the following manner. First one total feed current I_{feed} was fed to the circuit; then by attaching a voltmeter to each of the junctions,

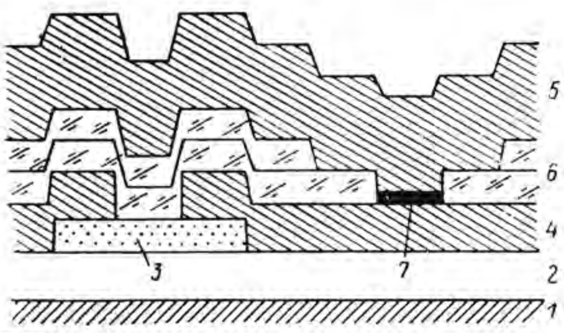

FIG. 5. Schematic section of a segment of the investigated structure.

it was possible to determine the values of the feed currents $(I_{feed})_i$ for which a nonzero voltage appeared on the i^{th} junction. then, setting I_{feed} at a level approximately 20% below the lowest of the values $(I_{feed})_i$, we measured the parameters of the interferometer. For this purpose, two additional currents I_{24} and I_{23} were sent through, independently of the total current I_{feed}. The current I_{24} was sent through between the currents I_2 and I_4 (Fig. 2), and the current I_{23} – between the currents I_2 and I_3. The critical value of the current I_{24} was then measured from the current I_{23}, which generates an additional flux through the inteferometer. The obtain curves correspond well to the known dependence of the critical current of a two-contact interferometer on the magnetic flux.[17] The working point of the interferometer was then identified by fixing the currents I_{23} and I_{24}. The magnitude of I_{23} was set in such a way as to minimize the critical value of I_{24}, and the current I_{24} itself was set to be less than this critical value by a magnitude of the order of half the modulation depth of the dependence of the critical current of the interferometer on the flux. Such a choice of the working point ensured identical conditions for the two stable states of the interferometer.

After tuning the interferometer to the generator G, the current I_{in} was fed to the circuit and the voltages at all the points of the circuit were mea-

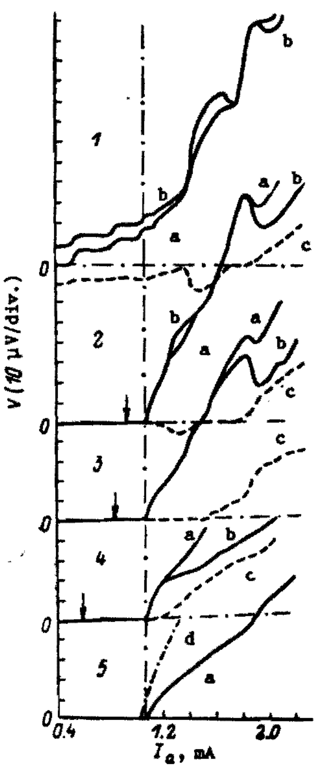

FIG. 6. Dependences of the voltages at two neighboring junctions (G and A_1) on the current in junction a for fixed values of the current in junction b: I_b = 1.05 (1), 0.95 (2), 0.85 (3), 0.6 (4), and 0.0 mA (5). The curves labeled c are the difference of V_b on the current I_b for I_a = 0.

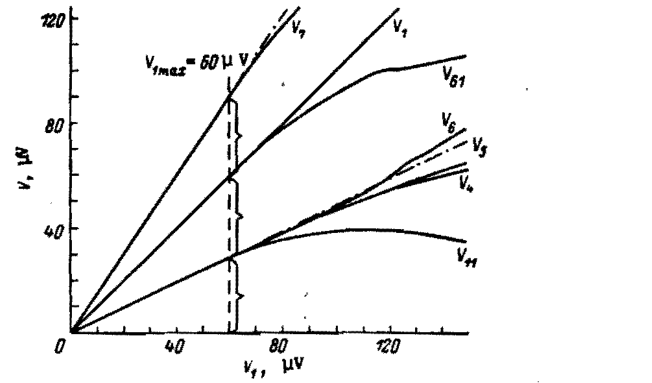

FIG. 7. Experimentally measured dependences of the voltages at the various points of the circuit on the voltage V_1 at the generator, obtained by slowly varying the generator current I_{in}.

sured. As the need arose, an additional tuning of the feed currents of the individual junctions was performed to ensure the fulfilment of relations (2) (actually, no more than two to three tunings were required to ensure the correct operation of the circuit).

Several samples, prepared according to the same technique, but differing in the magnitude of their critical current density j_c, were measured according to the above-described technique. Correct operation of the circuit could be observbed on practically all of the samples, but only within a narrow voltage region near zero (roughly up to 5 μV). An analysis of the experimental data showed that at low values of the critical current density $j_c \approx$ 0.2-0.3 kA/cm² as a result of the strong shunting of the junctions the operation of the combiner A_4 was unsatisfactory, as seen by the fact that it reproduced two closely adjacent pulses (Fig. 3c) incorrectly. To improve the operation of this circuit element, a sample with larger critical currents ($j_c \approx$ 0.5 kA/cm²) was prepared; however, in this case the normalized inductance L_3 of the interferometer turned out to be close to 5, i.e., substantially greater than the nominal value.[1,3] In order to decrease this inductance, an insulating layer of A2-1350 photoresist of thickness ~0.5 μm and a lead film screen of thickness ~500 nm were deposited over the entire sample. As a result, the characteristic value LI_c/Φ_0 of the interferometer was decreased to 2.5 and the working range was substantially extended.

Figure 7 shows experimental voltage relations at various points of the circuit which were measured by slowly varying the generator current I_{in} to the sample with a screen. It can be seen that relations (2) are fulfilled (at least with an experimental accuracy better than 0.5%) all the way to $V_1 \approx$ 60 μV, which corresponds to a repetition frequency of the single-quantum pulses being generated of f ≈ 30 GHz. As both experiment and numerical modeling show, at this frequency only the operating regime of the combiner A_4 breaks down, but the NOR gate and the delay line (J_4, J_5, J_6, J_{55}, J_{62}) can operate at even higher frequencies.

For this reason we carried out an additional experiment for the special purpose of verifying the workability of the NOR gate at high frequencies. In this experiment we tuned only the elements of the interferometer and the delay line and made measurements of the voltages on the elements J_4, J_5, J_6, J_{55}, and J_{62} as a function of the voltage V_{34} on the interferometer, which was measured between the points V_3 and V_4 (fig. 2). The voltages were varied as before by varying the current I_{in} of the generator; however, this measurement scheme did not allow us to account for the processes of pulse transmission in the part of the circuit that does not lead to the NOR gate. In such a regime it was possible to observe the correct operation of the NOR gate in the voltage range from V_{34} = 73 μV (the initial pulse frequency was ≈ 35 GHz) to $V_{34} \approx$ 98 μV (frequency ≈ 48 GHz).

We also carried out preliminary investigations of permissible deviations of the circuit parameters from their nominal values. At an initial pulse frequency of ~10 GHz the circuit remained in the correct operating regime for deviations of the feed current of ±2.5%.

CONCLUSION

In this paper we have demonstrated the workability of a test circuit containing the basic elements of a resistive single-quantum logic at frequencies up to 50 GHz. This result was achieved in a very simply constructed (and far from optimal) circuit containing only two superconducting layers, which were configures by lithographic techniques. The photolithography was carried out with a very moderate resolution (minimal layout dimensions of ∿10 μm). However, even in this case it was possible to achieve a frequency significantly higher than in other superconducting logic circuits, and somewhat better than the record results which have been achieved with GaAs circuits of similar complexity.[18]

Our theoretical estimates show that with the help of currently available circuit-design technology it should be possible to increase the clock frequency of the simplest devices up to 400 GHz, and the permissible spread of the parameters to ±20-30%.

The authors would like to thank Zh. I. Alferov, K. A. Valiev, and E. P. Velikhov for helpful discussions.

[1] K. Nakajima, Y. Onodera, and Y. J. Ogawa, Appl. Phys. 47, 1620 (1976).
[2] T. A. Fulton, R. S. Dynes, and P. W. Anderson, Proc. IEEE 61, 28 (1973).
[3] K. K. Likharev, IEEE Trans. Magn. MAG-13, 245 (1977).
[4] K. K. Likharev, S. V. Rylov, and V. K. Semenov, IEEE Trans. Magn. MAG-21, 947 (1985).
[5] A. H. Silver, R. R. Phillips, and R. D. Sandell, IEEE Trans. Magn. MAG-21, 204 (1985).
[6] K. Nakajima, G. Oya, and Y. Sawada, IEEE Trans. Magn. MAG-19, 1201 (1983).
[7] O. A. Mukhanov and V. K. Semenov, Preprint MGU No. 9, Moscow (1985).
[8] K. K. Likharev, O. A. Muchanov, and V. K. Semenov, in: SQUID'85, W. de Gruyter (ed.), Berlin (1985), p. 1103-1108.
[9] J. P. Hurrel, D. C. Pridmore-Brown, and A. H. Silver, IEEE Trans. Electron Devices ED-27, 1887 (1980).
[10] C. A. Hamilton and F. L. Lloyd, IEEE Electron Devices Lett. EDL-3, 335 (1982).
[11] A. N. Vystavkin, V. P. Koshelets, K. K. Likharev, et al., Pis'ma Zh. Tekh. Fiz. 13, 286 (1987) [Sov. Phys. Tech. Phys. Lett. 13, 117 (1987)].
[12] V. K. Semenov, A. A. Odintsov, and A. B. Zorin, in: SQUID'85, W. de Gruyter (ed.), Berlin (1985), p. 71.
[13] P. Wolf, in: The Josephson Effect – Achievements and Trends, A Barone (ed.), Naples (1985), pp. 449-463.
[14] M. Gurvitch, M. A. Washington, H. A. Huggins, and J. M. Rowell, IEEE Trans. Magn. MAG-19, 791 (1983).
[15] A. N. Vystavkin, V. P. Koshelets, G. A. Ovsyannikov, et al., Pis'ma Zh. Tekh. Fiz. 11, 290 (1985) [Sov. Tech. Phys. Lett. 11, 119 (1985)].
[16] A. K. Jain, K. K. Likharev, J. E. Lukens, and J. E. Sauvageau, Phys. Rep. 109, 309 (1984).
[17] K. K. Likharev, Introduction to the Dynamics of Josephson Junctions [in Russian], Nauka, Moscow (1985).
[18] M. Abe, T. Mimura, K. Nishiuchi, et al., IEEE Quant. Electron. QE-22, 1870 (1986).

Translated by P. F. Schippnick

Control of liquid-crystal correctors in adaptive optical systems

V. A. Dorezyuk, A. F. Naumov, and V. I. Shmal'gauzen

M. V. Lomonosov State University, Moscow

(Submitted December 14, 1987)

Zh. Tekh. Fiz. 59, 35–41 (December 1989)

Four means of control of a liquid-crystal wave-front corrector with one degree of freedom are considered: amplitude control, pulse control, and two types of amplitude–pulse control. Experimental characteristics of adaptive interferometers are presented.

In adaptive optical systems compensation of phase distortions of monochromatic radiation caused by turbulence of the propagation medium or by the optical system itself is realized, as a rule, by deformable mirrors.[1,2] The use for this purpose of liquid-crystal (LC) correctors can be advantageous in a number of cases.[3] Methods of control which use such correctors have their own peculiarities and to a significant degree determine the dynamic range of the adaptive system as a whole.

In the present paper we present results of experimental studies of methods of control using one channel of a LC corrector with electric addressing in a system with feedback. For this purpose we used a nematic liquid crystal cell whose operation is based on the electrooptical S-effect.[4] The technology of fabrication of such cells has been described in detail in Ref. 5.

AMPLITUDE CONTROL

Usually the required magnitude of the phase delay Φ for an ordinary light beam in the LC layer is achieved by varying the effective value of the voltage U applied to this layer. The behavior of $\Phi(U, t)$ for $U \leq 1.22U_0$ is described by the following expression:

$$\Phi(U, t) = \Phi_m \left\{1 - \frac{1}{8}\left(\frac{n_\parallel^2}{n_\perp^2} + \frac{n_\parallel}{n_\perp}\right)(U^2 - U_0^2)\left(\frac{2}{3}U^2 + \frac{K_{33} - K_{11}}{K_{11}} U_0^2\right)^{-1}\left[1 + \tanh\left(\frac{t - \tau_0}{\tau}\right)\right]\right\}. \quad (1)$$

Here $U_0 = \pi(4\pi K_{11}/\Delta\varepsilon)^{1/2}$ is the threshold voltage: $\Phi_m = 2\pi(n_\parallel - n_\perp)L/\lambda$ is the maximum value of the phase delay; K_{11} and K_{33} are the elastic moduli of transverse and longitudinal bending, respectively, of the LC molecules: $\Delta\varepsilon$ is the dielectric anisotropy; L is the thickness of the LC layer;

